A Novel Two-Quadrant Zero-Voltage Transition Converter for DC Motor Drives

K.T. Chau, T.W. Ching, C.C. Chan, and David T.W. Chan*
Department of Electrical and Electronic Engineering,
The University of Hong Kong, Pokfulam, HONG KONG
*Department of Electrical and Communications Engineering,
Hong Kong Technical College, Tsing Yi, HONG KONG

Abstract — A novel zero-voltage-transition (ZVT) two-quadrant (2Q) converter for dc motor drives is presented. It possesses the definite advantage that both main transistors and rectifiers can operate with zero-voltage switching in both motoring and regenerating modes, while both of these switches are only subjected to unity voltage and current stresses, namely the same as its PWM counterparts. This converter is particularly useful for dc traction systems in which both motoring and regenerative braking are desired to have high efficiency. The corresponding theoretical analysis and its high-efficiency performance are supported by both simulation and experimental results.

I. INTRODUCTION

Nowadays, the use of low-inductance dc motors is becoming attractive because of the advantages of higher power density, lower rotor inertia, smoother commutation and lower manufacturing costs. However, it usually suffers from high current ripples, resulting in increased losses and switching stresses. To alleviate this problem, the switching frequency of power converters needs to be increased from less than one to over one hundred kilohertz. With available power devices technologies, hard-switching PWM converters operating at such high frequencies impose high switching losses and switching stresses.

Recently, a number of soft-switching techniques, providing zero-voltage switching (ZVS) or zero-current switching (ZCS) conditions, have been successfully developed for switched-mode power supplies (SMPS) [1]-[4]. Surprisingly, the development of soft-switching converters for dc motor drives has been very little. Even so, it has been assumed that those being developed for SMPS can be directly applicable [5]. Until recently, a systematic evaluation of available soft-switching converters for dc motor drives has been carried out [6]. As a result, these soft-switching converters cannot satisfy the operating requirements of dc motor drives. Apart from suffering excessive voltage and current stresses, they cannot handle bidirectional power flow during regenerative braking.

Different to SMPS, dc motor drives, especially in traction applications, needs regenerative braking. Technically, the dc motor operates as a generator to convert the kinetic energy into the electrical energy while the converter must allow for bidirectional power flow to restore the energy to the power networks or battery systems. This energy-recovery feature is particularly attractive to electric railways and battery-powered electric vehicles.

In this paper, a novel ZVS-PWM, so-called zero-voltage transition (ZVT), 2Q converter for dc motor drives is proposed. Its principle of operation, characteristics curves in both the motoring and regenerative modes, design example, as well as simulation and experimental results will be given.

II. PRINCIPLE OF OPERATION

Fig. 1 shows the circuit diagram of the proposed ZVT-2Q soft-switching converter for dc motor drives. It differs from a conventional PWM-2Q converter, since the addition of a resonant inductor Lr, a resonant capacitor Cr and two auxiliary switches Sa and Sa'.

Since the operating characteristics of the proposed converter are generally dictated by those resonant elements, the corresponding characteristics impedance Z and angular frequency ω are defined as:

$$Z = \sqrt{\frac{Lr}{Cr}} \tag{1}$$

$$\omega = \sqrt{\frac{1}{Lr\,Cr}} \tag{2}$$

During the motoring and regenerating modes, the normalized motor currents are differently defined and expressed by (3)-(4) and (5)-(6), respectively:

$$I_N = \frac{V_g}{Z} \tag{3}$$

$$\lambda = \frac{I_o}{I_N} \tag{4}$$

$$I_N = \frac{V_o}{Z} \tag{5}$$

$$\lambda = \frac{I_g}{I_N} \tag{6}$$

The operating waveforms in the motoring mode are shown in Fig. 2, while the corresponding topological modes are illustrated in Fig. 3. Similarly, the operating waveforms in the regenerating mode are shown in Fig. 4, while the corresponding topological stages are illustrated in Fig. 5. As shown in Figs. 3 and 5, both modes exist seven operating stages within one switching cycle.

0-7803-3932-0

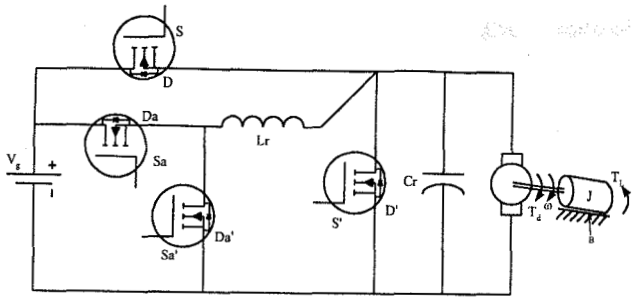

Fig. 1. Proposed ZVT-2Q converter.

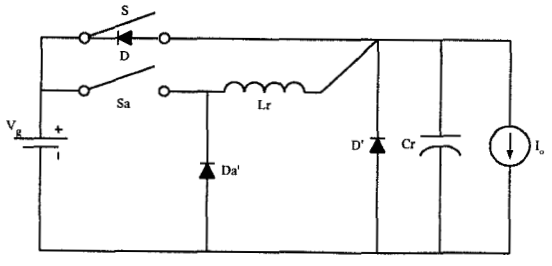

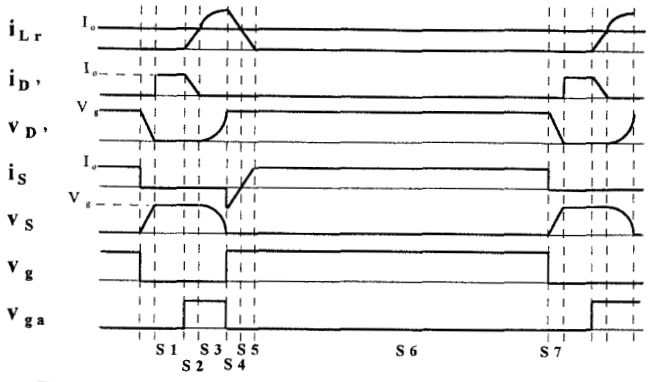

Fig. 2. Equivalent circuit and key waveforms during motoring mode.

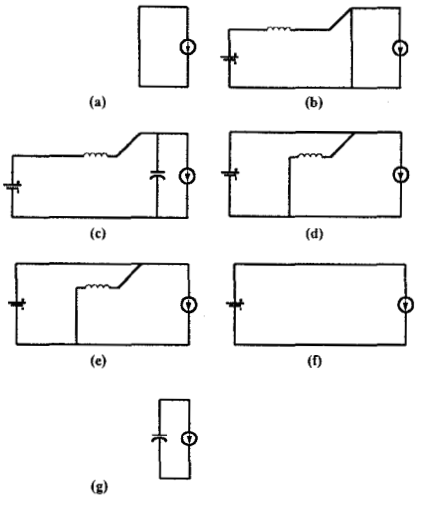

Fig. 3. Seven topological stages during motoring mode.

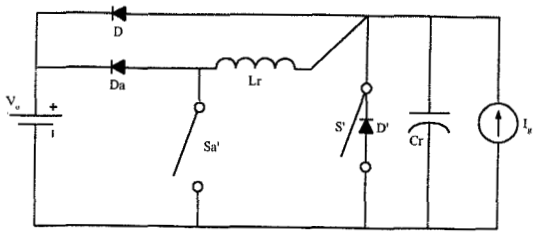

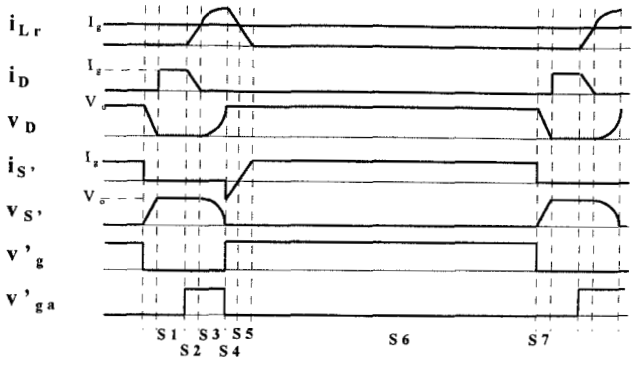

Fig. 4. Equivalent circuit and key waveforms during regenerating mode.

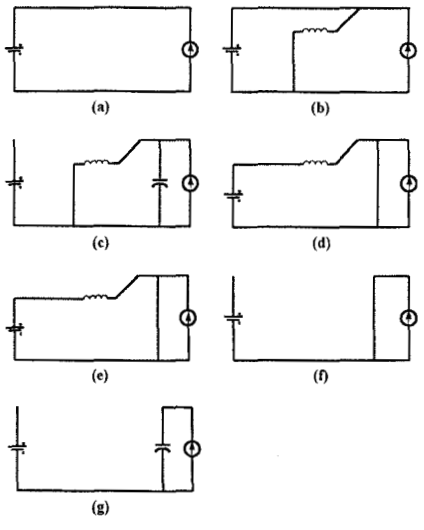

Fig. 5. Seven topological stages during regenerating mode.

A. *Motoring Mode (Figs. 2 & 3)*

(a) Stage 1 [T_0-T_1]: It is a freewheeling mode via D'.

(b) Stage 2 [T_1-T_2]: S_a is turned on. i_{Lr} increases according to the slope of V_g/Lr, with zero initial conditions $i_{Lr}(0)=0$ and $v_{D'}(0)=0$. i_{Lr} can be expressed as:

$$i_{Lr}(t) = \frac{V_g}{Lr} t \qquad (7)$$

This stage finishes at time T_2 when i_{Lr} equals I_o. The duration can be determined from (7) as given by:

$$T_2 = \frac{I_o Lr}{V_g} \tag{8}$$

(c) Stage 3 [T_2-T_3]: When $i_{Lr}=I_o$, D' is turned off with ZVS, and Lr and Cr start resonating. i_{Lr} and $v_{D'}$ are given by:

$$i_{Lr}(t) = I_N \sin\omega t + I_o \tag{9}$$

$$v_{D'}(t) = V_g(1-\cos\omega t) \tag{10}$$

v_{Cr} or $v_{D'}$ increases resonantly up to V_g at T_3 while $i_{Lr}=I_o+I_N$, and the duration can be determined by solving (10) as given by:

$$T_3 = \frac{\pi}{2\omega} \tag{11}$$

(d) Stage 4 [T_3-T_4]: When v_{Cr} or $v_{D'}$ reaches V_g, S is turned on with ZVS. S_a is turned off to recover the stored energy in Lr to the source. Then i_{Lr} flows through D_a' and decreases linearly with a slope of V_g/Lr. i_{Lr} can be expressed as:

$$i_{Lr}(t) = I_o + I_N - \frac{V_g}{Lr}t \tag{12}$$

i_{Lr} decreases to I_o at T_4 and the duration can be determined from (12) as given by:

$$T_4 = \frac{I_N Lr}{V_g} \tag{13}$$

(e) Stage 5 [T_4-T_5]: i_{Lr} keeps decreasing while i_S increasing until i_{Lr} reaches zero at T_5 and D_a' becomes off. During this stage, i_{Lr} is expressed as:

$$i_{Lr}(t) = I_o - \frac{V_g}{Lr}t \tag{14}$$

Since i_{Lr} decreases to zero at T_5, the duration can be determined by solving (14) which gives:

$$T_5 = \frac{I_o Lr}{V_g} \tag{15}$$

(f) Stage 6 [T_5-T_6]: It is a powering mode.

(g) Stage 7 [T_6-T_7]: I_o discharges Cr linearly with a slope of I_o/Cr until v_D' equals zero at T_7, and eventually D' becomes conducting. During this stage, v_D' can be expressed as:

$$v_{D'}(t) = V_g - \frac{I_o t}{Cr} \tag{16}$$

Again, T_7 can be determined by solving (16), which gives:

$$T_7 = \frac{V_g Cr}{I_o} \tag{17}$$

B. *Regenerating Mode (Figs. 4 & 5)*

(a) Stage 1 [T_0-T_1]: D is conducting, a regenerating mode.

(b) Stage 2 [T_1-T_2]: S_a' is turned on. i_{Lr} increases with the slope of V_o/Lr, while $i_{Lr}(0)=0$ and $V_{D'}(0)=V_o$. i_{Lr} can be expressed as:

$$i_{Lr}(t) = \frac{V_o}{Lr}t \tag{18}$$

This stage finishes at time T_2 when i_{Lr} equals I_g. The duration can be determined using (18) and is given by:

$$T_2 = \frac{I_g L_r}{V_o} \tag{19}$$

(c) Stage 3 [T_2-T_3]: When i_{Lr} reaches I_g at T_2, D is turned off with ZVS, and Lr and Cr start resonating. i_{Lr} and $V_{D'}$ are given by:

$$i_{Lr}(t) = \frac{V_o}{Z}\sin\omega t + I_g \tag{20}$$

$$v_{D'}(t) = V_o \cos\omega t \tag{21}$$

v_{Cr} or $v_{D'}$ decreases to zero at T_3, and the duration can be determined by solving (21) as given by:

$$T_3 = \frac{\pi}{2\omega} \tag{22}$$

(d) Stage 4 [T_3-T_4]: When $v_{S'}$ reaches zero, S' is turned on with ZVS. S_a' is turned off to recover the stored energy in Lr to the source. Then i_{Lr} flows through D_a and decreases linearly, which can be expressed as:

$$i_{Lr}(t) = I_g + I_N - \frac{V_o}{L_r}t \tag{23}$$

i_{Lr} decreased to I_g at T_4 and the duration can be determined by solving (23) which gives:

$$T_4 = \frac{I_N Lr}{V_o} \tag{24}$$

(e) Stage 5 [T_4-T_5]: i_{Lr} keeps decreasing and $i_{S'}$ increasing until i_{Lr} reaches zero at T_5. D_a becomes off. During this stage, i_{Lr} can be expressed as:

$$i_{Lr}(t) = I_g - \frac{V_o}{Lr}t \tag{25}$$

i_{Lr} decrease to zero at T_5 and the duration can be determined by solving (25) which gives:

$$T_5 = \frac{I_g Lr}{V_o} \tag{26}$$

(f) Stage 6 [T_5-T_6]: It is a freewheeling mode.

(g) Stage 7 [T_6-T_7]: I_g charges Cr linearly with a slope of I_g/Cr until v_D' equals V_o at T_7, and eventually D becomes conducting. During this stage, v_D' can be expressed as:

$$v_{D'}(t) = V_o - \frac{I_g t}{Cr} \tag{27}$$

Again, T_7 can be determined by solving (27) and is given by:

$$T_7 = \frac{V_o Cr}{I_g} \tag{28}$$

III. CHARACTERISTICS CURVES

A. Motoring Mode

The voltage-conversion ratio μ_m in the motoring mode of operation can be derived by averaging v_{Cr} or $v_{D'}$.

For Stage 3, integrating (10) and using (11):

$$v_{D'}(T_3) = V_g(\frac{\pi-2}{2\omega}) \tag{29}$$

For Stage 7, integrating (16) and using (17):

$$v_{D'}(T_7) = V_g(\frac{V_g Cr}{2I_o}) \tag{30}$$

Also, we define the duty ratio $\delta_m=T_{4-6}$ and T_3 as:

$$T_3 = \frac{T_s}{x} \tag{31}$$

$$T_s = \frac{x\pi}{2\omega} \tag{32}$$

where T_s is the switching frequency.

Hence, by using (1), (3)-(4) and (29)-(32), the voltage-conversion ratio μ_m can be expressed as:

$$\mu_m = \delta_m + \frac{\pi-2}{x\pi} + \frac{1}{x\pi\lambda} \tag{33}$$

The corresponding results showing the voltage conversion ratio μ_m versus load λ and duty cycle δ_m during the motoring mode are shown in Figs. 6 and 7, respectively.

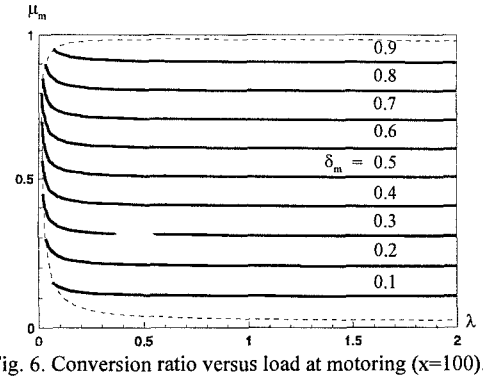

Fig. 6. Conversion ratio versus load at motoring (x=100).

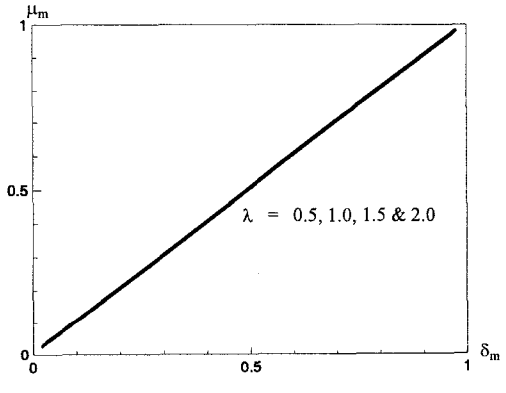

Fig. 7. Conversion ratio versus duty ratio at motoring (x=100).

B. Regenerating Mode

The voltage-conversion ratio μ_r in the regenerating mode can be derived by equating the source energy per cycle E_s and the output energy per cycle E_o:

$$E_S = V_s I_g T_S \tag{34}$$

$$E_o = V_o\left[i_D(T_1) + i_D(T_2) + i_{Lr}(T_4) + i_{Lr}(T_5)\right] \tag{35}$$

For stage 2, from (18) and (19):

$$i_D(T_2) = \frac{I_g^2 Lr}{2V_o} \tag{36}$$

For Stage 4, from (23) and (24):

$$i_{Lr}(T_4) = \frac{I_g I_N Lr}{V_o} + \frac{I_g^2 Lr}{2V_o} \tag{37}$$

For stage 5, from (25) and (26):

$$i_{Lr}(T_5) = \frac{I_g^2 Lr}{2V_o} \tag{38}$$

From (35) to (38):

$$E_o = V_o\left[I_g(T_1) + \frac{I_g^2 L_r}{2V_o} + \frac{I_g I_N L_r}{V_o} + \frac{I_N^2 L_r}{2V_o} + \frac{I_g^2 L_r}{2V_o}\right] \tag{39}$$

By equating (34) and (39) and defining the duty ratio $\delta_r=T_{5-6}$:

$$\mu_r = \frac{1}{1-\delta_r - \frac{\pi-2}{x\pi} - \frac{1}{x\pi\lambda}} \tag{40}$$

The corresponding results are shown in Figs. 8 and 9.

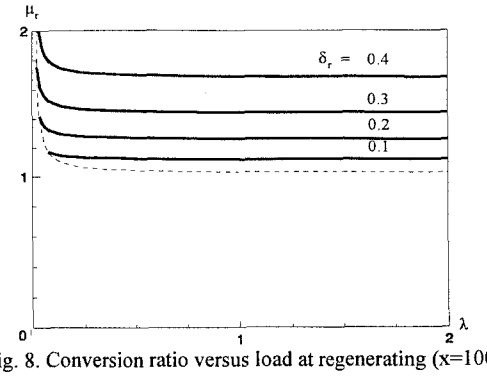

Fig. 8. Conversion ratio versus load at regenerating (x=100).

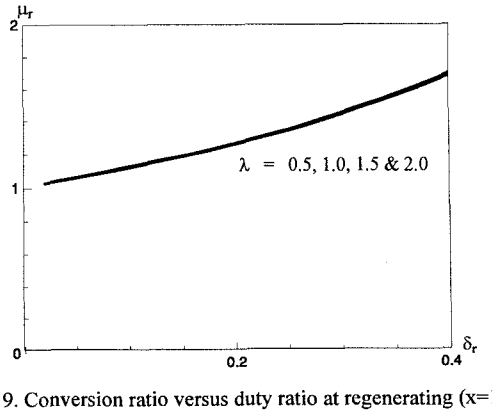

Fig. 9. Conversion ratio versus duty ratio at regenerating (x=100).

From (33) and (40), it can be shown that:

$$\mu_r = \frac{1}{1-\mu_m} \tag{41}$$

which is the same relation for conventional PWM buck and boost converters.

IV. DESIGN EXAMPLE

In order to illustrate the design process, a design example of the proposed ZVT-2Q converter for dc motor drives is carried out. With the specifications V_g=55-60V, V_o=50V, I_o=1-4A, T_s=10μs, x=100, the values of Lr and Cr are selected such that the resonant peak current is about one-half of the maximum load current. Thus, I_N=2A. From (1)-(3) and (32), we can deduce that Z=30Ω, ω=15.71×10^{6}rad/s (2.5MHz), Cr=2.12nF and Lr=1.91μH.

V. SIMULATION AND EXPERIMENTAL RESULTS

To verify the theoretical results, the ZVT-2Q converter with the parameters obtained in the design example is PSpice-simulated and hardware prototyped. From simulation results shown in Figs. 10 and 11, main transistors (i_S, v_S in Fig. 10 and $i_{S'}$, $v_{S'}$ in Fig. 11) and rectifiers (i_D, $v_{D'}$ in Fig. 10 and i_D, v_D in Fig. 11) operate with ZVS in both motoring and regenerating modes, and they are subjected to the same voltage and current stresses as those in the PWM counterpart. From the experimental waveforms shown in Figs. 12 and 13, they closely agree with those theoretical waveforms, especially the main switches (S and D' for motoring while S' and D for regenerating) can always maintain ZVS operation. As shown in Figs. 14-17, the characteristics curves are verified for different voltage conversion ratios and loads. Moreover, as shown in Fig. 18, the measured efficiency η of the proposed converter is quite high, ranging from 94% to 98%.

VI. CONCLUSION

A novel ZVT-2Q converter for dc motor drives has been presented. It possesses some definite advantages, including ZVS for all main switches and diodes, unity device voltage and current stresses, simple circuit topology and low cost, leading to achieve high switching frequency, high power density and high efficiency. Other key features are the use of the same resonant tank for both forward and backward power flows and the full utilization of all built-in diodes of the power switches, thus minimizing the overall hardware count and cost.

VII. ACKNOWLEDGMENT

This work was supported and funded in part by the Committee on Research and Conference Grants, the University of Hong Kong.

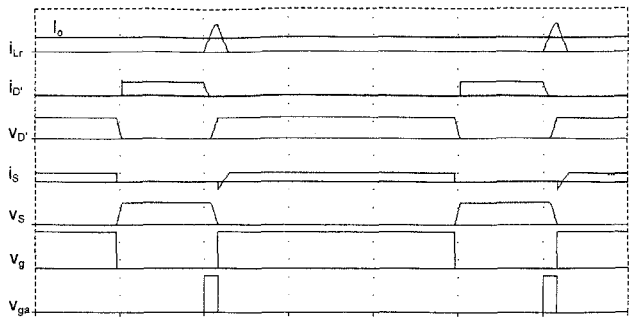

Fig. 10. PSpice simulation at motoring mode (δ_m=0.7).

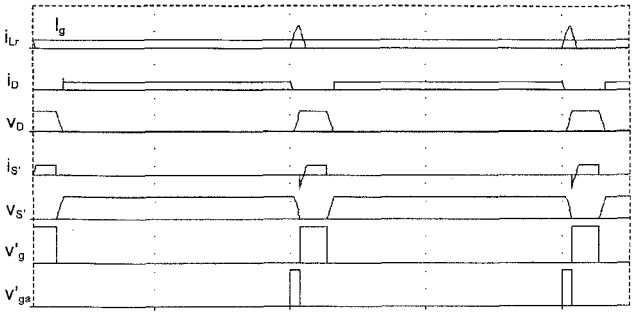

Fig. 11. PSpice simulation at regenerating mode (δ_r=0.1).

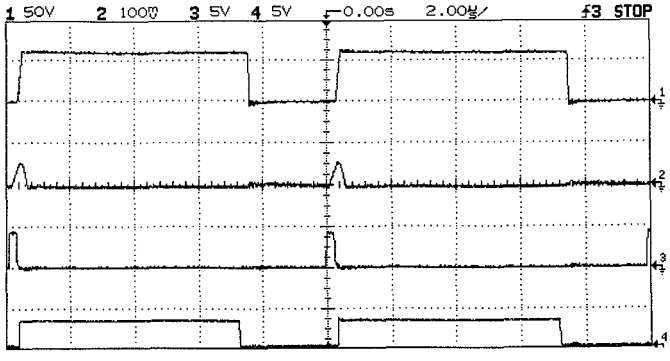

Fig. 12. Measured waveforms at motoring (δ_m=0.7); $v_{D'}$ (50V/div); i_{Lr} (10A/div), v_{ga}, v_g (5V/div).

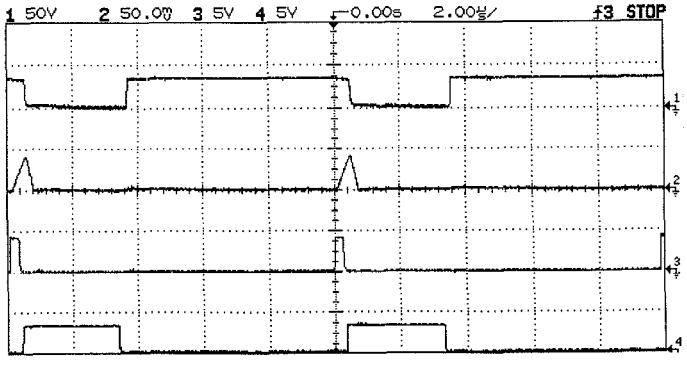

Fig. 13. Measured waveforms at regenerating (δ_r=0.3); $v_{S'}$ (50V/div); i_{Lr} (5A/div), v_{ga}', v_g' (5V/div).

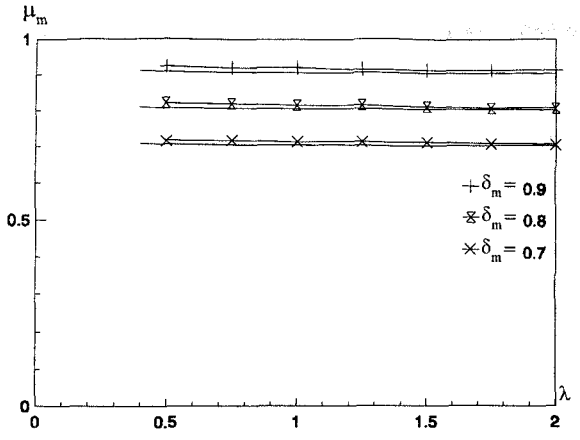

Fig. 14. Theoretical and experimental μ_m vs λ at motoring.

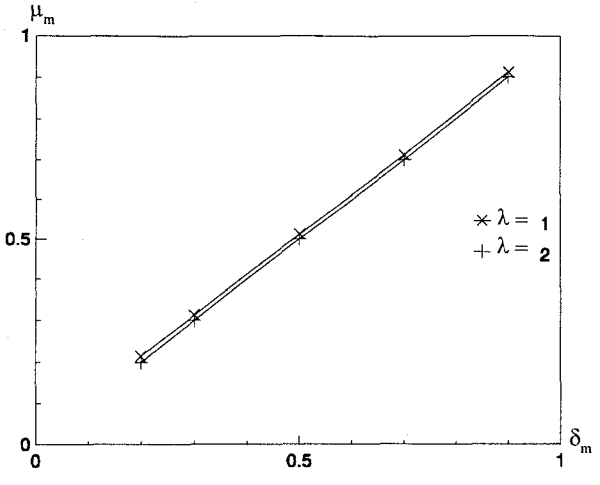

Fig. 15. Theoretical and experimental μ_m vs δ_m at motoring.

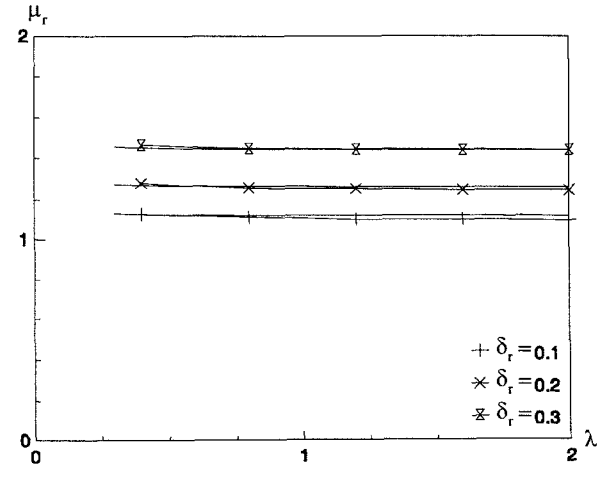

Fig. 16. Theoretical and experimental μ_r vs λ at regenerating.

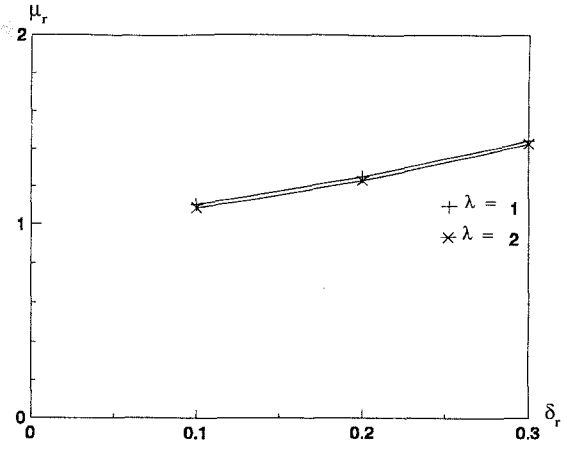

Fig. 17. Theoretical and experimental μ_r vs δ_r at regenerating.

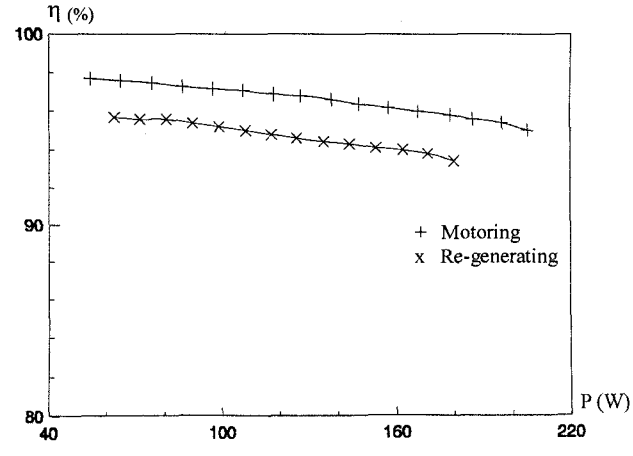

Fig. 18. Measured efficiency η at both motoring and regenerating.

VIII. REFERENCES

[1] D. Maksimović and S. Ćuk, "Constant-frequency control of quasi-resonant converters," *IEEE Trans. Power Electron.*, vol. 6, 1991, pp. 141-150.

[2] C.C. Chan and K.T. Chau, "A new zero-voltage-switching dc/dc boost converter," *IEEE Trans. Aero. Electron. Syst.*, vol. 29, 1993, pp. 125-134.

[3] G. Hua, C.S. Leu and F.C. Lee, "Novel zero-voltage-transition PWM converters," In *Proceedings of VPEC Power Electronics Seminar*, 1991, pp. 81-88.

[4] J.G. Cho, J.W. Baek, G.H. Rim and I. Kang, "Novel zero voltage transition PWM multi-phase converters," In *Proceedings of IEEE APEC*, 1996, pp. 500-506.

[5] C.C. Chong, C.Y. Chan and C.F. Foo, "A quasi-resonant converter-fed dc drive system," In *Proceedings of EPE*, 1993, pp. 372-377.

[6] K.T. Chau, T.W. Ching and C.C. Chan, "Constant-frequency multi-resonant converter-fed dc motor drives," In *Proceedings of IECON*, 1996, pp. 78-83.